NASA TECHNICAL NOTE

NASA TN D-3058

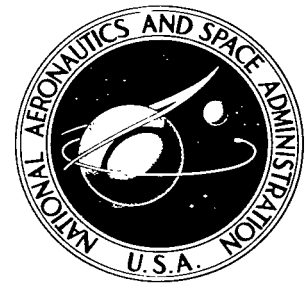

NASA TN D-3058

A SINGLE-COLLISION MODEL FOR ELECTRON-BEAM CURRENTS BETWEEN PLANE ELECTRODES

by Charles M. Goldstein and Arthur W. Goldstein

Lewis Research Center
Cleveland, Ohio

NATIONAL AERONAUTICS AND SPACE ADMINISTRATION - WASHINGTON, D. C. - NOVEMBER 1965

A SINGLE-COLLISION MODEL FOR ELECTRON-BEAM CURRENTS BETWEEN PLANE ELECTRODES

By Charles M. Goldstein and Arthur W. Goldstein

Lewis Research Center
Cleveland, Ohio

NATIONAL AERONAUTICS AND SPACE ADMINISTRATION

For sale by the Clearinghouse for Federal Scientific and Technical Information
Springfield, Virginia 22151 – Price $1.00

A SINGLE-COLLISION MODEL FOR ELECTRON-BEAM CURRENTS BETWEEN PLANE ELECTRODES*

by Charles M. Goldstein and Arthur W. Goldstein

Lewis Research Center

SUMMARY

Space-charge and potential distributions are calculated for the region between two plane electrodes. The effect of elastic, hard-sphere collisions between the electrons of the injected beam and the neutral gas molecules is incorporated into the analysis with the assumption that the electrons will suffer at most one scattering collision. The injected beam, itself, is assumed monoenergetic. Calculations of current as a function of voltage are compared with results from a multiple-collision model; very good agreement is found for an electrode-spacing to mean-free-path ratio of 0.1, and a maximum deviation of only 1.5 percent was observed for a ratio of 0.5. Current-voltage characteristics are also calculated for various values of emission current and electrode spacing. Collisions are found to have a pronounced influence on potential and density distributions, current, and region of time-independent operation.

INTRODUCTION

An important problem in the study of gaseous electronics and ionic phenomena is to find a means of analyzing the effect of collisions for those circumstances wherein they cannot be neglected but where a diffusion approximation is not yet applicable. This intermediate regime is of major importance in the low density plasma diode, the plasma sheath, the ion rockets, and the cross-sectional measurements. Presented herein is a simple, theoretical first approximation to the effect of collisions in this regime.

The particular problem treated is that of electron flow between plane parallel electrodes (emitter and collector) in the presence of an external electric field (see fig. 1) and collisions with a neutral target gas. The emitted electron beam is assumed monoenergetic and directed normal to the electrode surfaces. In addition, the following simplifying assumptions are made: the neutral gas particles are of infinite mass (perfect

*The material contained herein was presented at the Seventh International Conference on Phenomena in Ionized Gases, Belgrade, Yugoslavia, August 22-27, 1965.

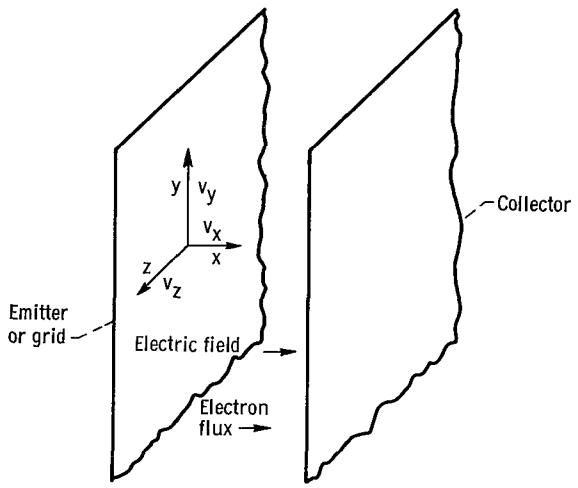

Figure 1. - Configuration of one-dimensional field, flux, and electrodes.

Lorentzian gas); electron-neutral collisions are elastic, hard-sphere collisions; and, the electrons suffer at most one scattering collision. The study is further restricted to the regime where a time-independent solution can be considered valid.

This single-collision model should provide good qualitative characteristics for a dilute gas; it will also provide a much-needed checkpoint for all future exact or approximate solutions of the more accurate physical models. The pursuance of this problem was in no small way influenced by the need for just such a checkpoint for a Monte Carlo problem (ref. 1). Not only did this model provide the needed checks for the Monte Carlo solution, but these latter solutions demonstrate, in turn, the range of validity of the one-collision approximation. A comparison of the results obtained from the two models will be discussed.

A review of the electron vacuum diode phenomena, which are of interest in the present study, is given in the following section. A more extensive review of research on monoenergetic electron flow in a vacuum diode is to be found in reference 2.

REVIEW OF COLLISIONLESS RESULTS

Figure 2 is a typical current-voltage characteristic obtained from a time-independent analysis (ref. 3) for the case of no collisions; figure 3 shows the corresponding potential distributions. As the collector voltage is decreased from A in figure 2, the full emission current reaches the collector until point B is reached. The curve labeled B in figure 3 represents the potential distribution corresponding to point B in figure 2. If the collector potential is now decreased infinitesimally, the potential minimum drops discontinuously to zero as indicated by curve B' in figure 3. This situation corresponds to point B' on the current-voltage characteristic (fig. 2). The point where the minimum potential and its slope are both zero is called a "virtual cathode." At this point, the ideal monoenergetic beam has zero velocity (infinite charge density). Other values of collector potential are determined by the amounts of the incident electron current that are reflected or transmitted at the virtual cathode. If the collector potential is now increased from, say, point C (fig. 2), a virtual cathode will continue to exist until point D is reached where the potential undergoes a discontinuous change and a normal potential minimum is once again formed (curve D', fig. 2).

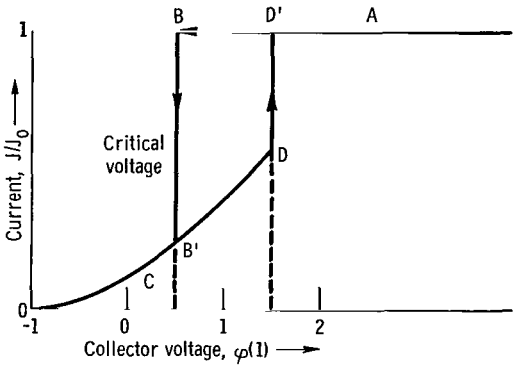

Figure 2. - Current-voltage characteristic; no collisions.

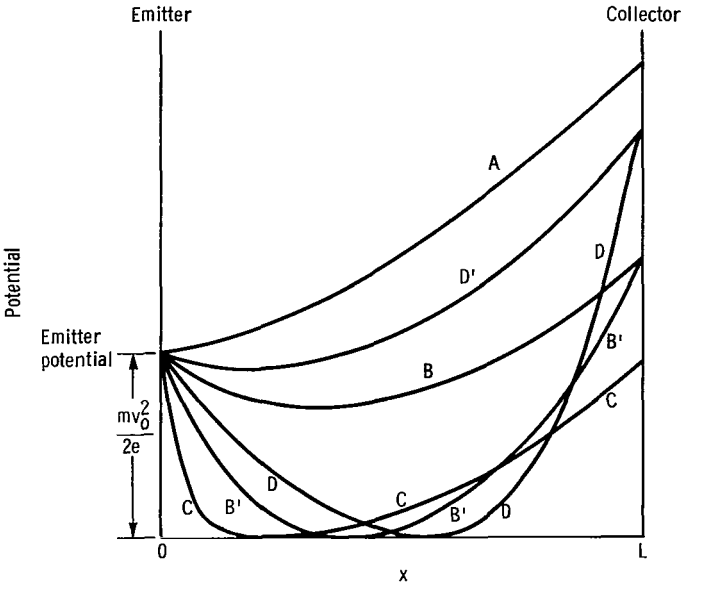

Figure 3. - Potential distributions; no collisions.

The hysteresis predicted by the collisionless current-voltage characteristics were not observed experimentally (ref. 4). More recently, the problem was simulated on a high-speed digital computor (ref. 5). The results indicate that a virtual cathode is never formed. Instead, for anode potentials below the critical potential (point B, fig. 2 and curve B, fig. 3), the potential minimum appears to oscillate nonuniformly with a period of roughly the order of the electron plasma frequency corresponding to the electron density at the potential minimum. Thus, in effect, only time-dependent solutions appear to exist below the critical potential.

ANALYSIS

Solutions to the single-collision problem are obtained by iteration in the following manner: an approximate potential distribution is first assumed for a given collector potential; the contribution of the electrons in the primary beam to the space charge is then easily calculated; the contribution of the scattered electrons is obtained from a solution of the Boltzmann transport equation; the total space charge is then employed, with Poisson's equation, to obtain a more accurate potential distribution. The entire process is iterated until sufficient accuracy is obtained.

Poisson's equation for the interelectrode region in dimensionless variables becomes

$$\varphi''(y) = C\,n(y) \tag{1}$$

where

$$\left.\begin{aligned} \varphi &\equiv \frac{2eV}{mv_o^2} \\ y &\equiv \frac{x}{L} \\ n(y) &\equiv \frac{N(y)}{\frac{J_o}{ev_o}} \\ C &= 8\pi \frac{e}{m} \frac{L^2 J_o}{v_o^3} \end{aligned}\right\} \tag{2}$$

(All symbols are defined in the appendix.) The parameter C is proportional to the strength of the space-charge effects. A low value of C indicates weak space-charge effects and vice versa.

The dimensionless charge density n(y) may be expressed as

$$n(y) = n_p(y) + n_s(y) \tag{3}$$

where $n_p(y)$ and $n_s(y)$ are the contributions to the charge density at y from the primary and scattered electrons, respectively.

Density of Electrons in Primary Beam

The assumption of hard-sphere collisions and a constant mean-free-path λ implies (see ref. 6)

$$N_p(x)v_p(x) = \frac{J_o}{e} e^{-x/\lambda} \tag{4}$$

where $N_p(x)$ is the density and $v_p(x)$ is the velocity of electrons in the primary beam (i. e., those electrons that have not been scattered). In this equation

$$v_p(x) = \sqrt{v_o^2 + \frac{2eV(x)}{m}} \tag{5}$$

and, therefore, from equations (2), (4), and (5),

$$n_p(y) = \frac{e^{-\kappa y}}{\sqrt{1 + \varphi(y)}} \tag{6}$$

where

$$\kappa \equiv \frac{L}{\lambda} \tag{7}$$

Equation (6) represents the density distribution of electrons in the primary beam.

Density of Scattered Electrons

Source intensity. - To solve Boltzmann's equation for the scattered electrons, the source intensity of scattered electrons is equated to the rate of loss of electrons from the primary beam. Equation (4) represents the flux of the primary beam electrons as a function of distance between the electrodes. The rate at which electrons are lost from the primary beam in distance dx is obtained by differentiating equation (4) with respect to x in the following way:

$$\frac{d}{dx} N_p(x)v_p(x) = - \frac{N_p(x)v_p(x)}{\lambda}$$

Hence the rate of loss of electrons from the primary beam per unit volume in phase space ($d\tau\, d\vec{v}$) is

$$\frac{N_p(x)v_p(x)}{\lambda} \delta(v_x - v_p)\delta(v_y)\delta(v_z) \tag{8}$$

Since hard-sphere scattering is energy conserving and isotropic, the rate of gain of scattered electrons per unit volume of phase space can be written in the form

$$R(x, v)\delta\left(v^2 - v_p^2\right) \tag{9}$$

When the gains and losses are equated (by integrating the integrals of eqs. (8) and (9) over the entire velocity space), there results

$$R(x, \vec{v}) = R(x) = \frac{N_p(x)}{2\pi\lambda} \tag{10}$$

Expressions (9) and (10) define the source intensity of the scattered electrons in phase space.

Equations for scattered electrons. - The Boltzmann transport equation for the scattered electrons with the derived collision term is

$$v_x \frac{\partial f(x, \vec{v})}{\partial x} + \frac{e}{m}\frac{dV}{dx}\frac{\partial f(x, \vec{v})}{dv_x} = \frac{N_p(x)}{2\pi\lambda}\delta\left(v^2 - v_p^2\right) \tag{11}$$

where $f(x, \vec{v})$ is the velocity distribution function of the scattered electrons. Integrating equation (11) with respect to v_y and v_z and nondimensionalizing result in

$$u\frac{\partial g(y, u)}{\partial y} + \frac{1}{2}\varphi'(y)\frac{\partial g(y, u)}{\partial u} = S(y) \tag{12}$$

where

$$\left.\begin{aligned} u &\equiv \frac{v_x}{v_o} \\ g(y, u) &\equiv \frac{v_o}{\frac{J_o}{ev_o}} \iint_{-\infty}^{+\infty} f(x, \vec{v})\, dv_y\, dv_z \\ S(y) &\equiv \frac{\kappa e^{-\kappa y}}{2\sqrt{1 + \varphi(y)}}, \qquad u^2 \le \frac{v_p^2}{v_o^2} \\ &\equiv 0, \qquad u^2 > \frac{v_p^2}{v_o^2} \end{aligned}\right\} \tag{13}$$

The dimensionless density of scattered electrons $n_s(y)$ is given by

$$n_s(y) = \int_{u_{min}}^{u_{max}} g(y,u)\,du \tag{14}$$

where $g(y,u)$ is a solution of equation (12) in the range bounded by u_{min} and u_{max} (which are themselves functions of y).

Solution of Boltzmann equation. - Equation (12) will be solved by the method of characteristics (ref. 7). After a collision has occurred, the normal velocity components v_y and v_z of each scattered electron are constant (no further collisions!); hence, the quantity

$$E \equiv u^2 - \varphi(y) \tag{15}$$

becomes a constant of motion of the scattered electrons. Transforming from the (y,u)-space to the (y,E)-space where

$$u = \pm\sqrt{E + \varphi(y)} \tag{16}$$

results in equation (12) becoming

$$u(y,E)\,\frac{\partial g}{\partial y}(y,E) = S(y) \tag{17}$$

Integration of equation (17) along constant E from a lower limit ξ to y gives

$$g(y,E) = g(\xi,E) + \int_{\xi}^{y} \frac{S(t)}{u(t,E)}\,dt \tag{18}$$

The bookkeeping becomes easier if the intermediate distribution functions $g_1^{\pm}(y,E)$ and $g_2^{\pm}(y,E)$ are employed

$$\left.\begin{aligned} g_1(y,E) &\equiv g(y \le y_m, E) = g_1^{+}(y,E) + g_1^{-}(y,E) \\ g_2(y,E) &\equiv g(y \ge y_m, E) = g_2^{+}(y,E) + g_2^{-}(y,E) \end{aligned}\right\} \tag{19}$$

where y_m is the location of the potential minimum, the $g_k^{+}(y,E)$ and $g_k^{-}(y,E)$ are the distribution functions for electrons with velocity $u \ge 0$ and $u \le 0$, respectively. From

equations (18) and (19)

$$g_k^{\pm}(y, E) = g_k^{\pm}(\xi, E) \pm \int_{\xi}^{y} K(t, E)\,dt \tag{20}$$

where

$$K(t, E) \equiv \frac{S(t)}{\sqrt{E + \varphi(t)}} \tag{21}$$

The boundary conditions at the electrodes, if perfect absorption is assumed, are

$$\left.\begin{aligned} g_1^{+}(0, E) &= 0 \qquad \text{(no scattering at emitter)} \\ g_2^{-}(1, E) &= 0 \qquad \text{(no scattering at collector)} \end{aligned}\right\} \tag{22}$$

Continuity of the distribution functions at the potential minimum is also demanded as shown in the following equation:

$$g_1^{\pm}(y_m, E) = g_2^{\pm}(y_m, E) \tag{23}$$

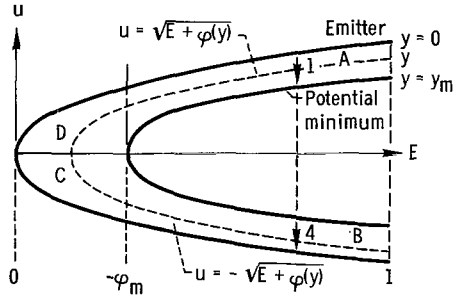

(a) $y \leq y_m$; region 1.

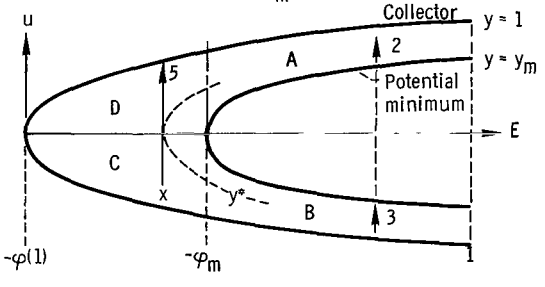

(b) $y \geq y_m$; region 2.

Figure 4. - Phase space of scattered electrons.

The integrals of equation (20) are to be evaluated along lines of constant E.

The limits of integration may be readily obtained with the aid of figure 4, which represents the phase space of scattered particles with E, u-axes. Contours of constant position (y = constant) are parabolas given by (cf. eq. (15))

$$u^2 = E + \varphi(y)$$

There are two regions in phase space; the first (fig. 4(a)) describes the region in physical space $0 \leq y \leq y_m$ where all the electrons are decelerated (in the vector sense), and the second (fig. 4(b)) describes the region in physical space $y_m \leq y \leq 1$ where all electrons are accelerated. In these diagrams, the paths of individual electrons are vertical lines (constant E) going

downward in region 1 (fig. 4(a)) and upward in region 2 (fig. 4(b)). The integrals of equation (20) are taken along the same paths.

The point of origin of a particle is determined by the location y of scattering and the axial velocity u after scattering. These determine the constant of motion E, which is always less than 1.0. The boundary conditions (eqs. (22)) imply $g = 0$ on $y = 0$, $u > 0$ (fig. 4(a)) and on $y = 1$, $u < 0$ (fig. 4(b)).

As an example, the trajectories of an electron starting near the emitter (represented by arrow 1 in fig. 4) shall be followed. This electron has a positive u-component of velocity as shown. Following a path of constant E toward the potential minimum, u decreases. After passing the potential minimum, the electron is accelerated toward the collector (arrow 2 in fig. 4(b)). Arrow 3 (fig. 4(b)) represents an electron with the same value of E but with a negative value of u resulting from a backscattering collision. The magnitude of u decreases until this electron traverses the potential minimum and is then accelerated into the emitter (arrow 4, fig. 4(a)).

Figure 4(a) also indicates that all electrons having positive u and $E < -\varphi_m$ in the region $y < y_m$ will be reflected by the potential field and returned to the emitter. Similarly, electrons with negative u and $E < -\varphi_m$ in the region $y > y_m$ (fig. 4(b)) will be reflected back to the collector. The trajectory of such an electron is represented by arrow 5 in figure 4(b). The value of y at which $u = 0$ is also indicated as y^*. Physically, this represents the turning point in the trajectory for a constant value of E due to the potential field.

With equations (20), (22), and (23), the following may be written for the indicated regions of figure 4:

$$g_{1a}(y, E) \equiv g_1^+(y, E \geq -\varphi_m) = \int_0^y K(t, E)dt \tag{24}$$

$$g_{1b}(y, E) \equiv g_1^-(y, E \geq -\varphi_m) = g_2^-(y_m, E \geq -\varphi_m) + \int_y^{y_m} K(t, E)dt \tag{25}$$

$$g_{1c}(y, E) \equiv g_1^-(y, E < -\varphi_m) = g_1^-(y^*, E < -\varphi_m) + \int_y^{y^*} K(t, E)dt \tag{26}$$

$$g_{1d}(y, E) \equiv g_1^+(y, E \leq -\varphi_m) = \int_0^y K(t, E)dt \tag{27}$$

$$g_{2a}(y, E) \equiv g_2^+(y, E \geq -\varphi_m) = g_1^+(y_m, E \geq -\varphi_m) + \int_{y_m}^y K(t, E)dt \tag{28}$$

$$g_{2b}(y, E) \equiv g_2^-(y, E \geq -\varphi_m) = \int_y^1 K(t, E)dt \tag{29}$$

$$g_{2c}(y, E) \equiv g_2^-(y, E \leq -\varphi_m) = \int_y^1 K(t, E)dt \tag{30}$$

$$g_{2d}(y, E) \equiv g_2^+(y, E \leq -\varphi_m) = g_2^+(y^*, E \leq -\varphi_m) + \int_{y^*}^y K(t, E)dt \tag{31}$$

Since the distribution functions must be continuous along constant E, the following may be equated from equations (27) and (30), respectively:

$$g_1^-(y^*, E \leq -\varphi_m) = g_1^+(y^*, E \leq -\varphi_m) = \int_0^{y^*} K(t, E)dt \tag{32}$$

$$g_2^+(y^*, E \leq -\varphi_m) = g_2^-(y^*, E \leq -\varphi_m) = \int_{y^*}^1 K(t, E)dt \tag{33}$$

Hence, equations (26) and (31) become

$$g_{1c}(y, E) = \int_0^y K(t, E)dt + 2\int_y^{y^*} K(t, E)dt \tag{34}$$

$$g_{2d}(y, E) = 2\int_{y^*}^y K(t, E)dt + \int_y^1 K(t, E)dt \tag{35}$$

Substituting equation (33) in equation (25) and equation (32) in equation (28) results in

$$g_{1b}(y, E) = \int_y^1 K(t, E)dt \tag{36}$$

$$g_{2a}(y, E) = \int_0^y K(t, E)dt \tag{37}$$

The limits on the integral in equation (14) can now be obtained in each region of the (y, E)-space by inspection of figure 4. For $y \leq y_m$, the respective contribution to the

densities becomes

$$n_{1a}(y) = \int_{\sqrt{\varphi(y)-\varphi_m}}^{\sqrt{1+\varphi(y)}} du \int_0^y K\left[t, u^2 - \varphi(y)\right] dt \tag{38}$$

$$n_{1b}(y) = \int_{\sqrt{\varphi(y)-\varphi_m}}^{\sqrt{1+\varphi(y)}} du \int_y^1 K\left[t, u^2 - \varphi(y)\right] dt \tag{39}$$

$$n_{1c}(y) = \int_0^{\sqrt{\varphi(y)-\varphi_m}} du \int_0^y K\left[t, u^2 - \varphi(y)\right] dt + 2 \int_0^{\sqrt{\varphi(y)-\varphi_m}} du \int_y^{y^*} K\left[t, u^2 - \varphi(y)\right] dt \tag{40}$$

$$n_{1d}(y) = \int_0^{\sqrt{\varphi(y)-\varphi_m}} du \int_0^y K\left[t, u^2 - \varphi(y)\right] dt \tag{41}$$

and for $y \geq y_m$,

$$n_{2a}(y) = \int_{\sqrt{\varphi(y)-\varphi_m}}^{\sqrt{1+\varphi(y)}} du \int_0^y K\left[t, u^2 - \varphi(y)\right] dt \tag{42}$$

$$n_{2b}(y) = \int_{\sqrt{\varphi(y)-\varphi_m}}^{\sqrt{1+\varphi(y)}} du \int_y^1 K\left[t, u^2 - \varphi(y)\right] dt \tag{43}$$

$$n_{2c}(y) = \int_0^{\sqrt{\varphi(y)-\varphi_m}} du \int_y^1 K\left[t, u^2 - \varphi(y)\right] dt \tag{44}$$

$$n_{2d}(y) = 2 \int_0^{\sqrt{\varphi(y)-\varphi_m}} du \int_{y^*}^y K\left[t, u^2 - \varphi(y)\right] dt + \int_0^{\sqrt{\varphi(y)-\varphi_m}} du \int_y^1 K\left[t, u^2 - \varphi(y)\right] dt \tag{45}$$

A straightforward change of the limits of integration may be affected for equations (38), (39), (41), (42), (43), and (44), and for those integrals of equations (40) and (45), which do not contain y^* as a limit. The integrals containing y^* can be inverted, however, by employing the following identity:

$$\int_0^L d\alpha \int_0^\alpha h(\alpha,\beta)d\beta = \int_0^L d\beta \int_\beta^L h(\alpha,\beta)d\alpha \tag{46}$$

The second integral of equation (40) may be written in the form

$$\int_0^{\varphi(y)-\varphi_m} d\alpha \int_0^\alpha h(\alpha,\beta)d\beta \tag{47}$$

where

$$\left.\begin{aligned} \sqrt{\alpha} &\equiv u \\ \beta(t) &\equiv -\varphi(t) + \varphi(y) \\ h(\alpha,\beta) &\equiv \frac{K\left[t,\ \alpha - \varphi(y)\right]}{\sqrt{\alpha}\ \beta'(t)} \end{aligned}\right\} \tag{48}$$

(Note that it has been assumed that $\varphi(t)$ is monotonic in the range of interest, hence $\beta'(t)$ and t may be expressed as functions of β.) Application of the identity (eq. (46)) to equation (47) gives

$$\int_0^{\varphi(y)-\varphi_m} d\beta \int_\beta^{\varphi(y)-\varphi_m} h(\alpha,\beta)d\alpha = 2\int_y^{y_m} dt \int_{\sqrt{\varphi(y)-\varphi(t)}}^{\sqrt{\varphi(y)-\varphi_m}} K\left[t, u^2 - \varphi(y)\right] du \tag{49}$$

The same procedure gives, for the first integral of equation (45),

$$2\int_{y_m}^{y} dt \int_{\sqrt{\varphi(y)-\varphi(t)}}^{\sqrt{\varphi(y)-\varphi_m}} K\left[t, u^2 - \varphi(y)\right] dt \tag{50}$$

After changing the order of integration in equations (38) to (45), the integration over u may be done in closed form. The indefinite integral is

$$\int K\left[t, u^2 - \varphi(y)\right] du = \int \frac{S(t)\,du}{\sqrt{u^2 - \varphi(y) + \varphi(t)}} = S(t) \ln \left| u + \sqrt{u^2 - \varphi(y) + \varphi(t)} \right| \tag{51}$$

Hence, integrating over u and collecting terms from equations (38) to (51) result in

$$n_s(y) = \int_0^{y_m} dt \cdot S(t) \ln \left| \frac{\sqrt{1 + \varphi(y)} + \sqrt{1 + \varphi(t)}}{\sqrt{\varphi(y) - \varphi_m} \mp \sqrt{\varphi(t) - \varphi_m}} \right|$$

$$+ \int_{y_m}^{1} dt \cdot S(t) \ln \left| \frac{\sqrt{1 + \varphi(y)} + \sqrt{1 + \varphi(t)}}{\sqrt{\varphi(y) - \varphi_m} \pm \sqrt{\varphi(t) - \varphi_m}} \right| \tag{52}$$

where the upper signs in the denominators pertain to $y \leq y_m$ and vice versa.

Current to Collector

To obtain the net collector current J, it is simpler to first obtain the net current to the emitter J_E

$$\frac{J_E}{J_o} = \int_{u \leq 0} u \cdot g_1(0, E)\,du \tag{53}$$

or

$$\frac{J_E}{J_o} = \int_{u \leq 0} u \left[g_{1b}(0, E) + g_{1c}(0, E) \right] du \tag{54}$$

from equations (25) and (26). Substituting equations (34) and (36) into equation (54) and referring to figure 4 (p. 8) for the proper limits result in

$$\frac{J_E}{J_o} = \int_0^{\sqrt{-\varphi_m}} du \cdot u \int_0^{y^*} 2K(t, u^2)\,dt + \int_{\sqrt{-\varphi_m}}^{1} du \cdot u \int_0^{1} K(t, u^2)\,dt \tag{55}$$

Inverting the order of integration (using eq. (46) for first term in eq. (55)) and integrating with respect to u give

$$\frac{J}{J_o} = 1 - \frac{J_E}{J_o} = \frac{1}{2}\left(1 + e^{-\kappa}\right) - \int_0^{y_m} S(t)\sqrt{\varphi(t) - \varphi_m}\, dt + \int_{y_m}^{1} S(t)\sqrt{\varphi(t) - \varphi_m}\, dt \qquad (56)$$

RESULTS

The equations for the electron density distribution were solved simultaneously with Poisson's equation for the potential distribution and current. Solutions were obtained for several values of the space-charge parameter (C = 0. 1, 1, and 10) and the collision parameter (L/λ = 0, 0. 1, 0. 3, and 0. 5). For each pair of parameters, the collector potential was varied from a large positive value down to the neighborhood of the critical potential.

Case 1 (C = 10)

Figure 5 shows the overall current-voltage curves for high space-charge conditions and several values of L/λ. For comparison, the results of the Monte Carlo calculation are shown, where multiple collisions are allowed but also limited to hard-sphere elastic collisions. The one-collision approximation yields collector currents that are accurate for L/λ = 0. 1 and is accurate over most of the range for L/λ = 0. 3, but it is somewhat

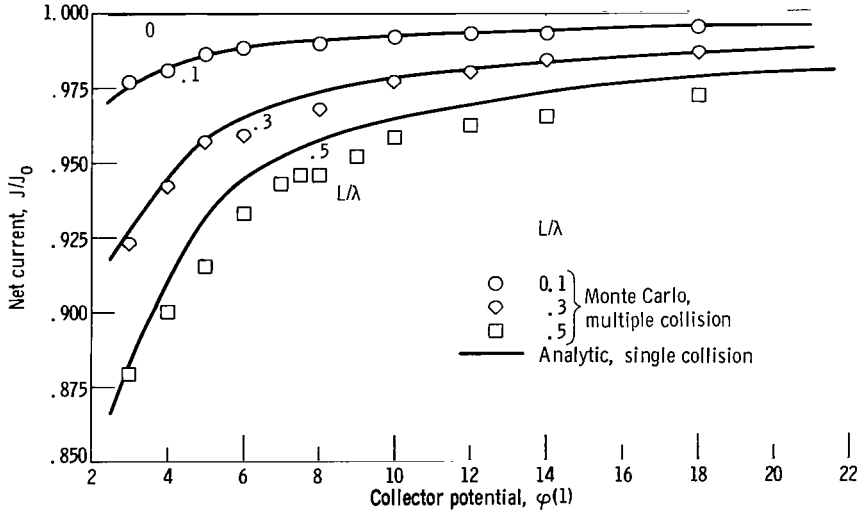

Figure 5. - Current-voltage characteristics; C = 10.

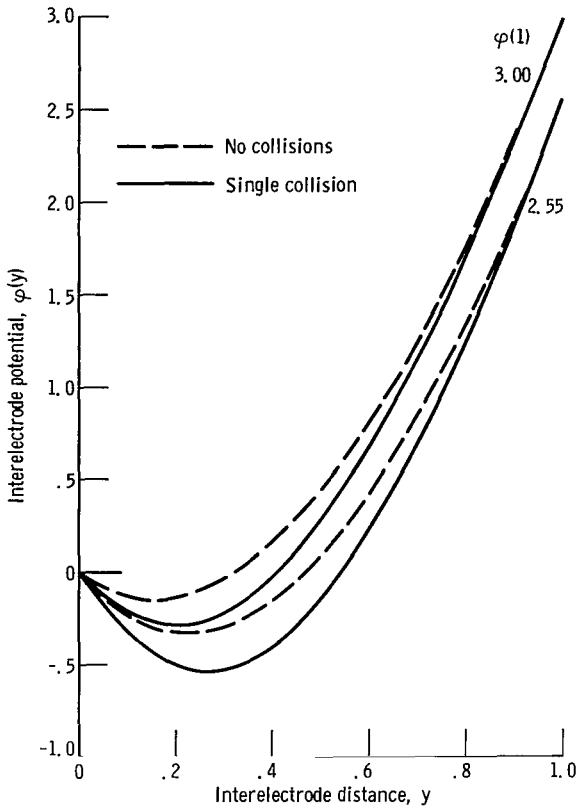

Figure 6. - Potential distributions near transition voltage; C = 10; L/λ = 0.5.

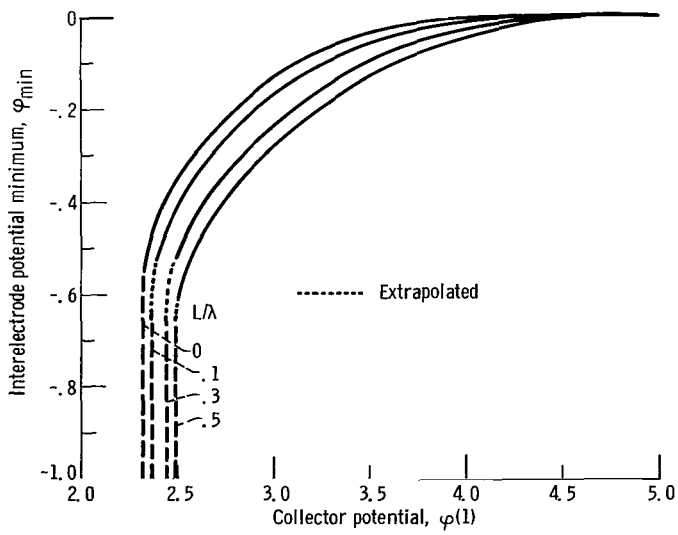

Figure 7. - Critical potential and minimum potential with mean-free-path; C = 10.

too high (by as much as 1.5 percent) for $L/\lambda = 0.5$. These curves show that collisions cause a backscattering of electrons to the emitter even for large collector voltages (J/J_o remains less than unity).

Typical potential distributions (shown in fig. 6) are qualitatively the same as those that exist without collisions. The only apparent effect of collisions is to lower the potential minimum for a given collector potential.

The effect of collisions on the critical collector potential and the corresponding potential minimum is shown in figure 7. The critical potential is defined at the point where the slope of the curve of potential minimum plotted against collector potential becomes infinite (ref. 4). It is observed that collisions reduce the range of stable operation by increasing the critical value of the collector potential. In addition, the corresponding potential minimum decreases.

The electron density distribution obtained by the one-collision method for $C = 10$ and $L/\lambda = 0.5$ is shown in figure 8. Curve C shows a distribution corresponding to an electrical field of zero at the emitter ($\varphi'(0) = 0$). In this case, the potential increases monotonically with y, the primary beam electrons accelerate, and their density decreases. Scattered electrons returning to the emitter increase the density there over the emitted value of 1.0. Density curve A corresponds to the lower potential distribution of figure 7;

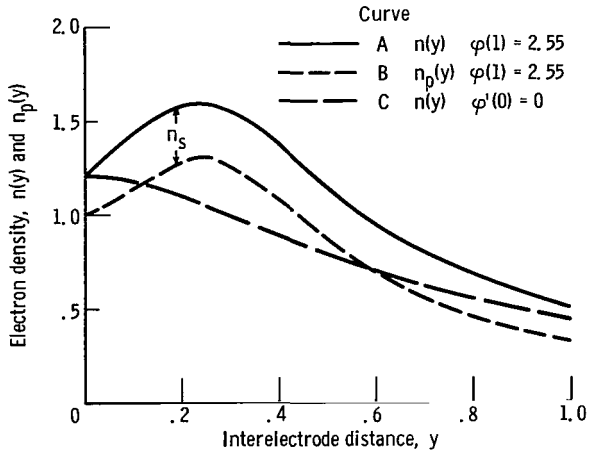

Figure 8. - Density distribution; C = 10; L/λ = 0.5.

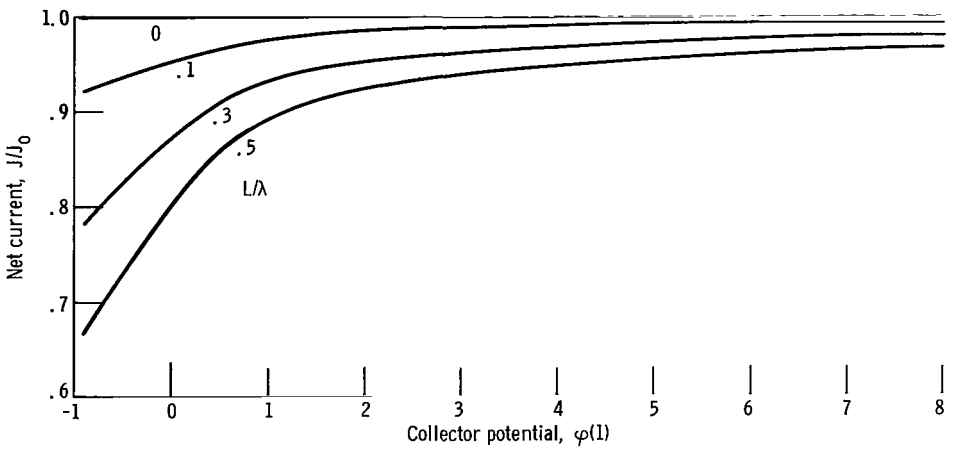

Figure 9. - Current-voltage characteristics; C = 1.

the maximum density location occurs in the neighborhood of the minimum potential distribution (viz., the minimum u-component of electron velocity). The curve labeled B shows the density distribution (n_p) of members of the primary beam for the same potential curve ($\varphi(1) = 2.55$). The density of scattered electrons (n_s) is seen to be in the range 0.17 to 0.29.

Case 2 (C = 1)

In this case the current-voltage curves (fig. 9) are qualitatively similar to those for case 1. Here, however, the critical potential is much lower ($\varphi(1) \approx -0.9$). Note that as the collector potentials become very high, the saturation currents for this case approach the values for case 1 (fig. 5). As the collector potential increases, the effect of the space charge decreases; the only mechanism, then, that maintains the saturation current

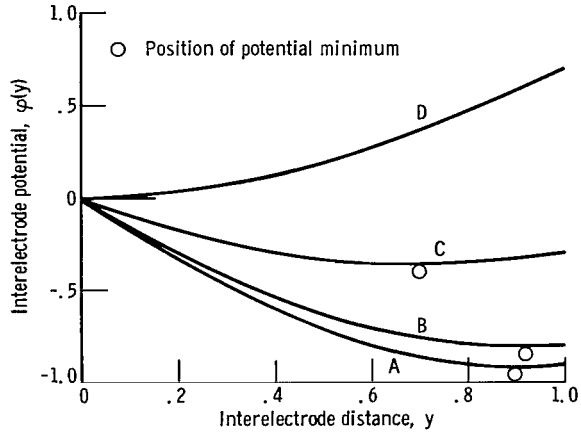

Figure 10. - Potential distribution; C = 1; L/λ = 0.5.

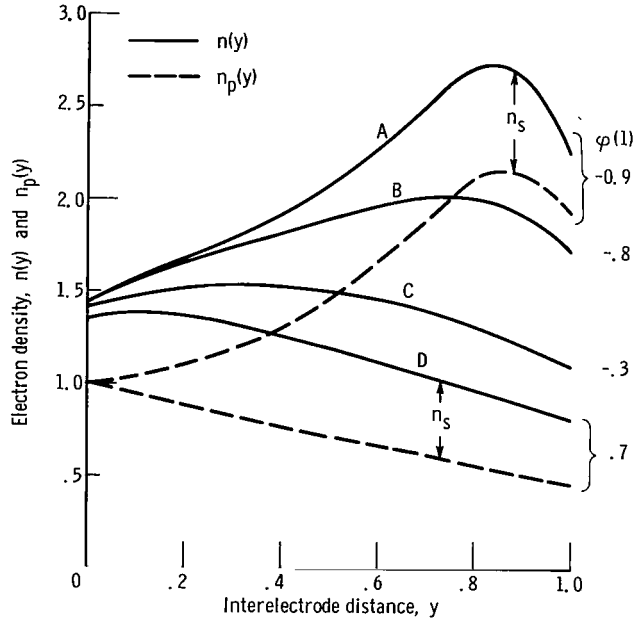

Figure 11. - Density distribution; C = 1; L/λ = 0.5.

below the emission current ($J/J_o = 1$) at very high collector potentials is the scattering.

The potential distributions for C = 1 and L/λ = 0.5 are shown in figure 10. As the collector potential $\varphi(1)$ is reduced in the sequence of curves D, C, B, and A, the potential minimum first approaches the collector, and then recedes, as indicated by the position of the circles in the figure. For this case the potential minimum never reaches the collector (i. e., the slope of the potential never becomes zero at the collector). The corresponding density distributions are shown in figure 11, where it is observed that for this value of C the scattering begins to dominate the space charge as is evidenced by the lack of correlation in positions of potential minimum and density maximum. The

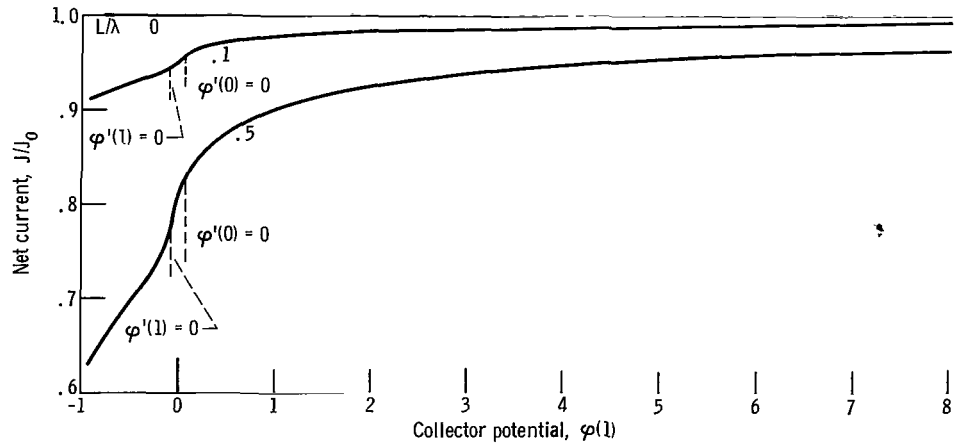

Figure 12. - Current-voltage characteristics; C = 0.1

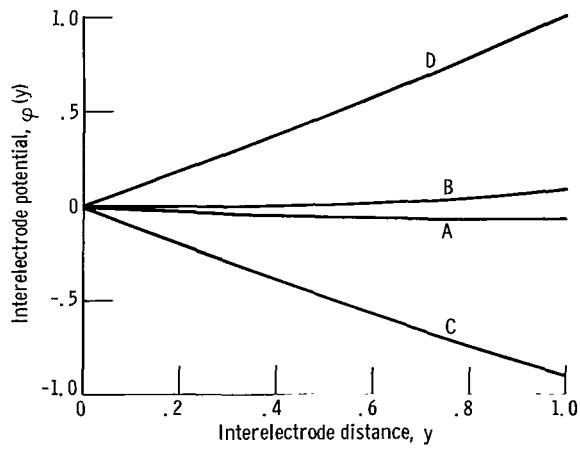

Figure 13. - Potential distribution; C = 0.1; L/λ = 0.5.

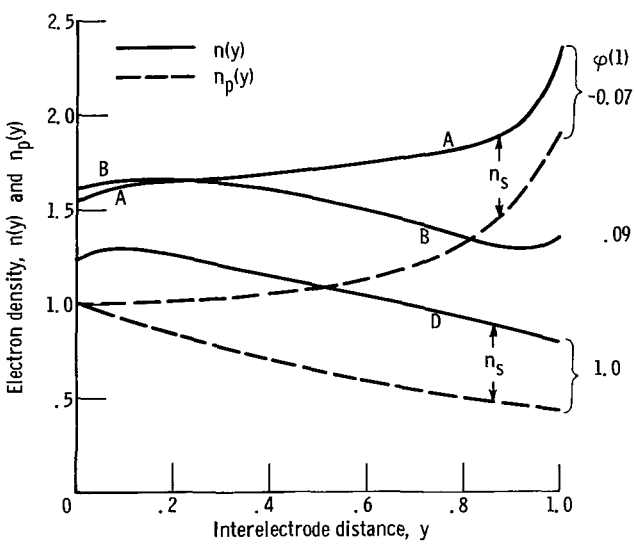

Figure 14. - Density distribution; C = 0.1; L/λ = 0.5.

density of the primary beam n_p is also shown for $\varphi(1) = -0.9$ and for $\varphi(1) = 0.7$.

Case 3 (C = 0.1)

Here, a qualitative change in the current-voltage curves (fig. 12) for collector potentials near $\varphi(1) = 0$ and lower is observed. The collector potentials coinciding with $\varphi'(1) = 0$ and $\varphi'(0) = 0$ define different regimes of operation as indicated by the corresponding potential distributions, curves A and B, in figure 13. The region between these two curves is known as the space-charge region. As the collector potential is decreased from that of curve B to that of curve A, the potential minimum moves from the emitter to the collector. Below curve A the potential minimum is located at the collector, and above curve B the potential minimum is located at the emitter. The almost linear potential distributions outside the space-charge region (curves C and D), and the small extent of the space-charge

region are indicative of weak space-charge effects (viz., small values of C.)

The density distribution n(y) of electrons, corresponding to the potential distributions of figure 13, is shown in figure 14. Here the scattering and acceleration are easily shown to have opposite effects on electron density. The distribution A corresponds to a greater number of electrons being reflected back to the emitter than does distribution B. Hence, in general, the electron density of A is higher. Near the emitter, however, the returning electrons of curve A are accelerated to a higher mean velocity than those of curve B, due to the higher electric fields. The increased mean velocity more than compensates for the higher back current, so that a net decrease in density results.

CONCLUSIONS

The calculations show that adequately accurate prediction of the effect of collisions on diode current-voltage characteristics are obtainable from the single-collision model if the spacing L is sufficiently small compared with the mean free path λ; errors of only 1.5 percent in current were obtained with $L/\lambda = 0.5$.

Backscattering of electrons causes a reduction in the current reaching the collector. This reduction becomes most pronounced at low collector potentials where the interaction between scattering and the space-charge effects are strongest. These effects are shown to be accentuated with increase in the magnitude of the space-charge parameter C. In addition, the scattering causes a slight reduction in the range of stable operation.

Lewis Research Center,
National Aeronautics and Space Administration,
Cleveland, Ohio, July 14, 1965.

APPENDIX - SYMBOLS

[Cgs units are used throughout.]

C	space-charge parameter, eq. (2)
E	constant of motion defined in eq. (15)
e	electronic charge
$f(x, \vec{v})$	velocity distribution function (v. d. f.) of scattered electrons
$g(y, E)$	dimensionless v. d. f. for scattered electrons, eq. (13)
$h(\alpha, \beta)$	variable defined in eq. (48)
J	net electron current to collector
J_E	net electron current to emitter
J_o	electron emission current
$K(t, E)$	kernel defined in eq. (21)
L	interelectrode spacing
m	electron mass
N(x)	electron density
n(y)	dimensionless electron density defined in eq. (2)
$R(x, v)$	source kernel, eq. (10)
S(y)	dimensionless source intensity defined in eq. (12)
u	dimensionless x-component of velocity, eq. (13)
V(x)	potential with respect to the emitter
$\vec{v}$	velocity, v_x, v_y, v_z
x	coordinate normal to electrode surfaces
y	dimensionless coordinate normal to electrode surfaces defined in eq. (2)
y*	value of y where u = 0 in integration along constant E, shown in fig. 4
α, β	variable of integration, eq. (51)
$\delta(x)$	Dirac Delta-function
κ	dimensionless mean-free-path defined in eq. (7)
λ	mean-free-path (mfp)
τ	volume
$\varphi(y)$	dimensionless potential defined in eq. (2)

Subscripts:

a, b, c, d	regions of fig. 4
m	value at potential minimum
max	maximum
min	mimimum
o	initial conditions (at emitter)
p	primary beam electrons
s	scattered electrons
1	$y \leq y_m$
2	$y \geq y_m$

Superscripts:

+	flow toward collector
-	flow toward emitter

REFERENCES

1. Goldstein, Charles M.: Monte Carlo Method for the Calculation of Transport Properties in a Low-Density Ionized Gas. NASA TN D-2959, 1965.

2. Ivey, H. F.: Space Charge Limited Currents. Advances in Electronics and Electron Physics. Vol. VI. Academic Press, Inc., 1954, p. 137.

3. Salzberg, B.; and Haeff, A. V.: Effects of Space Charge in the Grid-Anode Region of Vacuum Tubes. RCA Rev., vol. 2, no. 1, Jan. 1938, pp. 336-366; 374.

4. Bull, C. S.: Space-Charge Effects in Beam Tetrodes and Other Valves. J. Inst. Elec. Engrs. (London), pt. III, vol. 95, no. 33, Jan. 1948, pp. 17-24.

5. Birdsall, Charles K.; and Bridges, William B.: Space-Charge Instabilities in Electron Diodes and Plasma Converters. J. Appl. Phys., vol. 32, no. 12, Dec. 1961, pp. 2611-2618.

6. Kennard, E. H.: Kinetic Theory of Gases. McGraw-Hill Book Co., Inc., 1938.

7. Hildebrand, F. B.: Advanced Calculus for Engineers. Prentice-Hall, Inc., 1949, p. 368ff.

3/18/83

"The aeronautical and space activities of the United States shall be conducted so as to contribute . . . to the expansion of human knowledge of phenomena in the atmosphere and space. The Administration shall provide for the widest practicable and appropriate dissemination of information concerning its activities and the results thereof."

—NATIONAL AERONAUTICS AND SPACE ACT OF 1958

NASA SCIENTIFIC AND TECHNICAL PUBLICATIONS

TECHNICAL REPORTS: Scientific and technical information considered important, complete, and a lasting contribution to existing knowledge.

TECHNICAL NOTES: Information less broad in scope but nevertheless of importance as a contribution to existing knowledge.

TECHNICAL MEMORANDUMS: Information receiving limited distribution because of preliminary data, security classification, or other reasons.

CONTRACTOR REPORTS: Technical information generated in connection with a NASA contract or grant and released under NASA auspices.

TECHNICAL TRANSLATIONS: Information published in a foreign language considered to merit NASA distribution in English.

TECHNICAL REPRINTS: Information derived from NASA activities and initially published in the form of journal articles.

SPECIAL PUBLICATIONS: Information derived from or of value to NASA activities but not necessarily reporting the results of individual NASA-programmed scientific efforts. Publications include conference proceedings, monographs, data compilations, handbooks, sourcebooks, and special bibliographies.

Details on the availability of these publications may be obtained from:

SCIENTIFIC AND TECHNICAL INFORMATION DIVISION

NATIONAL AERONAUTICS AND SPACE ADMINISTRATION

Washington, D.C. 20546